

CO self-shielding as the origin of oxygen isotope anomalies in the early solar nebula

J. R. Lyons^{1,2} & E. D. Young^{1,2}

The abundances of oxygen isotopes in the most refractory mineral phases (calcium-aluminium-rich inclusions, CAIs) in meteorites¹ have hitherto defied explanation. Most processes fractionate isotopes by nuclear mass; that is, ¹⁸O is twice as fractionated as ¹⁷O, relative to ¹⁶O. In CAIs ¹⁷O and ¹⁸O are nearly equally fractionated, implying a fundamentally different mechanism. The CAI data were originally interpreted as evidence for supernova input of pure ¹⁶O into the solar nebula¹, but the lack of a similar isotope trend in other elements argues against this explanation². A symmetry-dependent fractionation mechanism^{3,4} may have occurred in the inner solar nebula⁵, but experimental evidence is lacking. Isotope-selective photodissociation of CO in the innermost solar nebula⁶ might explain the CAI data, but the high temperatures in this region would have rapidly erased the signature⁷. Here we report time-dependent calculations of CO photodissociation in the cooler surface region of a turbulent nebula. If the surface were irradiated by a far-ultraviolet flux $\sim 10^3$ times that of the local interstellar medium (for example, owing to an O or B star within ~ 1 pc of the protosun), then substantial fractionation of the oxygen isotopes was possible on a timescale of $\sim 10^5$ years. We predict that similarly irradiated protoplanetary disks will have H₂O enriched in ¹⁷O and ¹⁸O by several tens of per cent relative to CO.

Self-shielding of CO in the solar nebula is a process of isotope-selective photodissociation that occurs at far-ultraviolet (FUV) wavelengths from 91.2 nm to 110 nm. Because CO first goes to a bound excited state before dissociating, the absorption spectrum of CO consists of many narrow lines. The wavelength of each line is determined by the specific vibrational and rotational levels involved, and is shifted when the mass of the molecule is changed as a result of an isotopic substitution. The absorption spectra of the various CO isotopologues do not overlap significantly, particularly at the low temperatures of molecular clouds and the outer regions of the solar nebula. During photodissociation the most abundant isotopologue (C¹⁶O) saturates, which reduces its rate of dissociation relative to the less abundant C¹⁸O and C¹⁷O. This produces a zone of enrichment of ¹⁸O and ¹⁷O, and corresponding depletion of C¹⁸O and C¹⁷O.

Very large fractionations ($\sim 10^4\%$) are observed^{8,9} and predicted¹⁰ in diffuse and translucent molecular clouds, and it has recently been suggested¹¹ that H₂O produced by CO dissociation in the parent molecular cloud can explain oxygen isotope abundances in CAIs. Because large fractionations are not observed in cloud cores⁹, this mechanism implies that the solar nebula derived from cloud envelope material. However, star formation results from core collapse in dense molecular clouds, and it is unclear whether large fractionations in more tenuous clouds are inherited by protostellar nebulae.

Surface regions of the nebula are similar in temperature and pressure to dense molecular clouds, and are therefore a likely site for formation and preservation of oxygen isotope heterogeneity produced during self-shielding¹². To investigate the influence of

CO self-shielding on oxygen isotope ratios in the early Solar System, we used a one-dimensional photochemical model to compute the time-dependent oxygen isotope profiles in a two-dimensional, axisymmetric nebula. The total gas number density in the disk was specified with a standard analytical disk model¹³. For a nebula of bulk composition similar to the solar composition¹⁴, the initial volume fractions are $f_{\text{He}} = 0.16$, $f_{\text{CO}} = 2 \times 10^{-4}$, $f_{\text{H}_2\text{O}} = 2 \times 10^{-4}$ and $f_{\text{MgFeSiO}_4} = 2 \times 10^{-5}$, assuming that all C is in CO, all Si is in MgFeSiO₄, and all remaining O is in H₂O.

Disk photochemistry in the model is initiated by CO dissociation



where $x = 16, 17$ and 18 , and by H₂ and H photoionization at wavelengths less than 91.2 nm. Disk chemistry was restricted to H-, C- and O-containing chemical species, and the reaction rate coefficients used are a subset of the UMIST kinetics database¹⁵. By using previously published disk models^{13,16,17}, we developed a reduced set of 96 species and 375 reactions to model the disk chemistry. Gas-grain reactions are also included, using published desorption energies^{16,17}. Although our model is less sophisticated in its treatment of chemistry and radiative transfer than some recent models^{18,19}, it is, to our knowledge, the first model to include both vertical transport and oxygen isotopes.

To follow the time evolution and vertical distribution of O-containing species in the disk resulting from CO photodissociation high above the midplane, we solved the one-dimensional continuity equation for each species as a function of height above the midplane (see Supplementary Information). Vertical motion is characterized by a vertical diffusion coefficient, D_v , which is assumed to be comparable to the turbulent viscosity, $\nu_t = \alpha cH$, where c is the sound speed, H is the vertical scale height in the nebular gas, and $\alpha < 1$ is a parameter used in disk models to describe the strength of turbulent mixing²⁰. Theoretical models of disk instabilities²⁰ suggest that $\alpha \approx 10^{-3}$ to 10^{-1} . All quantities depend on r , the radial location in the disk, and so a value of r must be specified. We have chosen $r = 30$ AU (midplane temperature of 51 K) as representative of cold regions of the disk where water ice formation is expected.

To quantify the effects of self-shielding, we derived fits to numerically determined shielding functions developed for molecular clouds in the interstellar medium^{10,21} (see Supplementary Information). The photodissociation rate of each CO isotopologue is proportional to the product ϵJ_{ISM} , where $J_{\text{ISM}} = 2.0 \times 10^{-10} \text{ s}^{-1}$ is the rate constant for CO photolysis due to the local interstellar medium (LISM) FUV field¹⁰, and ϵ is an FUV flux enhancement factor. Dust opacity is identical for all isotopologues, and was parameterized in the same manner as is done for the interstellar medium. We consider a range of $\epsilon = 1$ to 10^5 , consistent with an FUV enhancement due to proximity to a massive O star in a star-forming region²².

Integration of the system of continuity equations yields the time evolution of species abundances in the model. Following CO

¹Institute of Geophysics and Planetary Physics, ²Department of Earth and Space Sciences, University of California, Los Angeles, California 90095, USA.

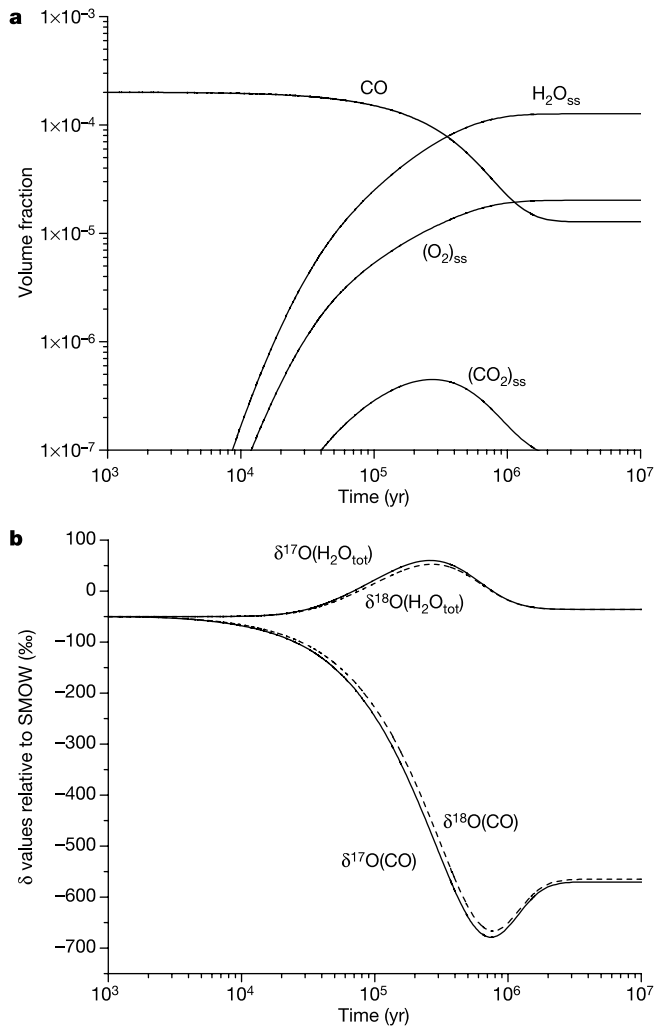


Figure 1 | Model results for the time evolution of molecular abundances and isotope ratios at the nebula midplane at a heliocentric distance of 30 AU. The temperature at the midplane is 51 K, and 0.1- μm dust particles are uniformly distributed in the gas. The turbulent viscosity parameter $\alpha = 10^{-2}$, consistent with previously published estimates^{20,26}. The FUV flux enhancement factor is $\epsilon = 500$ relative to the LISM flux, which implies a dust temperature of 110 K at the nebula surface. **a**, Volume fractions of several species relative to total nebular gas (the subscript 'ss' refers to O derived from CO self-shielding). C is ionized and forms a suite of hydrocarbon ions and molecules (not shown) as is predicted in other disk models¹⁷. **b**, $\delta^{17}\text{O}$ and $\delta^{18}\text{O}$ of CO and total nebular H_2O ($\text{H}_2\text{O}_{\text{tot}}$) relative to standard mean ocean water (SMOW). $\text{H}_2\text{O}_{\text{tot}}$ consists of $\text{H}_2\text{O}_{\text{ss}}$ plus H_2O from the parent molecular cloud, $\text{H}_2\text{O}_{\text{cloud}}$. The oxygen isotope δ -value for an unknown 'u' is computed as

$$\delta^x \text{O}_{\text{COinitial}}(\text{u}) = 10^3 \left(\frac{(x\text{O}/^{16}\text{O})_{\text{u}}}{(x\text{O}/^{16}\text{O})_{\text{COinitial}}} - 1 \right)$$

for all oxygen-containing molecules in the nebula, for $x = 17$ and 18. Initial CO in the nebula is assumed to have oxygen isotope ratios of $^{16}\text{O}/^{18}\text{O} = 500$ and $^{16}\text{O}/^{17}\text{O} = 2,600$. The δ -values are then converted from a 'CO initial' reference to a SMOW reference (see Supplementary Information), assuming that $\delta^x \text{O}_{\text{SMOW}}(\text{CO}_{\text{initial}}) = -50\text{‰}$, the measured value of the isotopically lightest CAIs. The oxygen isotope composition of total nebular H_2O is then given by the weighted sum of $\delta^x \text{O}_{\text{SMOW}}(\text{H}_2\text{O}_{\text{cloud}})$ and $\delta^x \text{O}_{\text{SMOW}}(\text{H}_2\text{O}_{\text{ss}})$, where the volume fraction of H_2O from the parent cloud is $f_{\text{H}_2\text{O}_{\text{cloud}}} = 2 \times 10^{-4}$ and the isotope composition of the H_2O in the cloud is $\delta^x \text{O}_{\text{SMOW}}(\text{H}_2\text{O}_{\text{cloud}}) = -50\text{‰}$.

self-shielding and dissociation, H_2O is formed by reactions of H and O on grain surfaces. The formation timescale for H_2O is $\sim 10^5$ years at the midplane for $\alpha = 10^{-2}$ and $\epsilon = 500$ (Fig. 1a). Total water in the nebula, $\text{H}_2\text{O}_{\text{tot}}$, consists of H_2O from the parent molecular cloud and the H_2O produced from O liberated during CO self-shielding, $\text{H}_2\text{O}_{\text{ss}}$. For comparison with meteorite oxygen isotope data, the model oxygen isotope ratios ($^{18}\text{O}/^{16}\text{O}$ and $^{17}\text{O}/^{16}\text{O}$) are expressed as δ -values ($\delta^{17}\text{O}_{\text{SMOW}}$ and $\delta^{18}\text{O}_{\text{SMOW}}$) relative to the isotope ratios in ocean water (see Fig. 1 legend). A difference of several hundred per mil is predicted between the $\delta^{17}\text{O}_{\text{SMOW}}$ and $\delta^{18}\text{O}_{\text{SMOW}}$ values of nebular H_2O and CO at times $> 10^4$ years (Fig. 1b). The non-mass-dependent isotope signature, $\Delta^{17}\text{O}_{\text{SMOW}} = \delta^{17}\text{O}_{\text{SMOW}} - 0.52 \delta^{18}\text{O}_{\text{SMOW}}$, is a useful quantity because it is unaffected by mass-dependent fractionation processes. An FUV flux enhancement of $\epsilon \approx 10^2$ – 10^3 yields $\Delta^{17}\text{O}_{\text{SMOW}}$ of $\text{H}_2\text{O}_{\text{tot}}$ in the range inferred from meteorites on timescales much less than the lifetime of gas in the nebula, which is $\sim 10^6$ – 10^7 years (Fig. 2).

Figure 3 shows the trajectory of $\delta^{17}\text{O}_{\text{SMOW}}$ and $\delta^{18}\text{O}_{\text{SMOW}}$ values of nebular water at the midplane for $\epsilon = 500$. The slope of the trajectory is ~ 5 – 10% too high compared to the slope-0.94 line² and slope-1.0 line²³ measured for CAIs. A slope > 1 is expected for self-shielding in pure CO because of the greater abundance, and therefore greater self-shielding, of C^{18}O compared to C^{17}O . Because CO dissociation occurs in an H_2 -rich environment, the wavelength dependence of H_2 absorption must be included in CO self-shielding calculations. About 60% of the dissociation of C^{18}O in molecular clouds occurs¹⁰

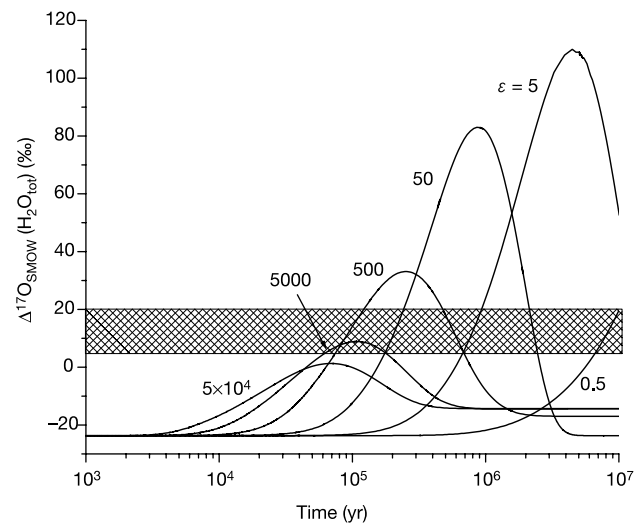


Figure 2 | The time evolution of the non-mass-dependent oxygen isotope component of total nebular H_2O for a range of FUV flux enhancement factors. Other parameters are as given in Fig. 1. The non-mass-dependent isotope signature is defined as $\Delta^{17}\text{O}_{\text{SMOW}} = \delta^{17}\text{O}_{\text{SMOW}} - 0.52 \times \delta^{18}\text{O}_{\text{SMOW}}$. The cross-hatched area indicates the range of minimum $\Delta^{17}\text{O}_{\text{SMOW}}$ inferred for total nebular H_2O from analyses of carbonaceous chondrites^{27–29}; higher $\Delta^{17}\text{O}_{\text{SMOW}}$ values of total nebula water are allowed by the meteorite data. For $\epsilon = 5, 50$ and 500 , $\Delta^{17}\text{O}_{\text{SMOW}}(\text{H}_2\text{O}_{\text{tot}})$ values at the midplane are within or above the cross-hatched region. Lower FUV fluxes do not photolyse enough CO within 1 Myr to produce sufficient fractionation at the midplane. For a given α , the maximum $\Delta^{17}\text{O}_{\text{SMOW}}(\text{H}_2\text{O}_{\text{tot}})$ decreases as FUV flux increases, suggesting that it may be possible to place an upper limit on the FUV incident upon the disk; for this case, the upper limit would be $\epsilon \approx 10^4$. The isotopic composition of nebular H_2O is also dependent on α . Results for $\alpha = 10^{-3}$ (not shown) are similar to $\alpha = 10^{-2}$, but timescales are ~ 3 times longer. For $\alpha = 10^{-4}$, weak mixing implies an insufficient turnover of CO to maintain efficient self-shielding, yielding $\Delta^{17}\text{O}_{\text{SMOW}}(\text{H}_2\text{O})$ well below the values inferred from meteorites. Thus, the value of $\Delta^{17}\text{O}_{\text{SMOW}}$ of nebular H_2O predicted by the model is sensitive to a key disk parameter, α , and to a key nebular environment parameter, the FUV flux incident on the disk.

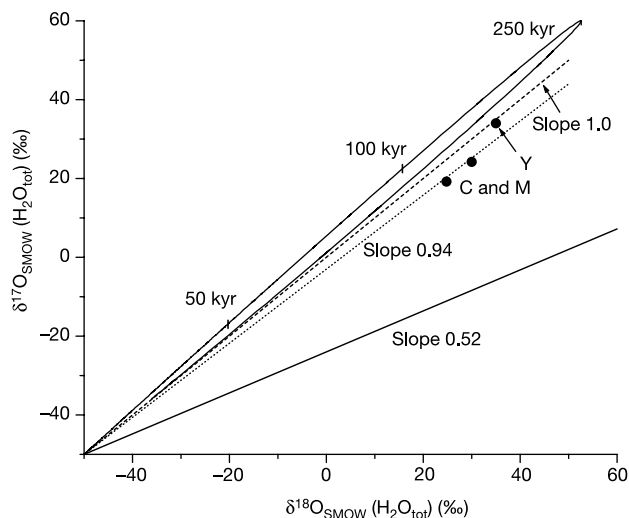


Figure 3 | Three-isotope plot ($\delta^{17}\text{O}_{\text{SMOW}}$ versus $\delta^{18}\text{O}_{\text{SMOW}}$) of total nebular H_2O at the midplane, with time labelled along the trajectory. Model parameters are as given in Fig. 1. 'Slope' is defined by the ratio $\delta^{17}\text{O}/\delta^{18}\text{O}$. The carbonaceous chondrite anhydrous mineral (CCAM) line^{1,2} (slope 0.94), which describes bulk CAIs, is shown for reference. A line of slope 1.00, measured in a particularly unaltered CAI of the Allende meteorite²³, and a mass-dependent fractionation line (slope 0.52), are also shown. The minimum isotopic composition of initial nebular H_2O as inferred from analyses of carbonaceous chondrites is indicated by 'C and M' (ref. 27) and 'Y' (ref. 29). The slope of the model trajectory is $\sim 10\%$ too high compared to the CCAM line, and $\sim 5\%$ higher than the slope-1.0 line. A similar slope was estimated³⁰ for self-shielding in pure O_2 . A slope > 1 is expected for the model trajectory, because although absorption by H_2 is accounted for (see Supplementary Information), the wavelength dependence of the overlap of H_2 absorption on CO isotopologue lines has not been included.

in a particular band of CO (band no. 31). Inclusion of H_2 absorption on band 31 (see Supplementary Information) brings the model slope into the range inferred for nebular water, and provides strong support for the self-shielding mechanism (Fig. 4).

Transfer of the non-mass-dependent signature in nebular water to the rocky component of the nebula requires H_2O to have been concentrated relative to CO in the disk midplane¹¹. Without concentration of H_2O at the midplane, equilibration of CO and H_2O as material migrated inward to $\sim 1\text{--}2\text{ AU}$ would have returned both CO and H_2O to the bulk isotopic values of the parent cloud. For the model presented here, concentration of ice-coated dust with $\Delta^{17}\text{O} > 0$ at the midplane implies grain growth timescales of $> 10^4$ years. Inward migration of ice-rich metre-sized objects may have then delivered ^{17}O and ^{18}O -rich water to the snowline²⁴. However, layered accretion²⁵ is likely to have been important in the ionized, self-shielding region of the disk, with the result that $\Delta^{17}\text{O}$ -rich water was deposited along the top of the disk dead zone (a predicted zone of weak mixing). Quantitative evaluation of oxygen isotopes in a layered accretion disk will require a two-dimensional chemical transport model.

We conclude that if CO self-shielding occurred primarily in the solar nebula, a strong FUV source was present ($\sim 10^3$ times LISM) and disk vertical mixing was vigorous ($\alpha \approx 10^{-2}$). An FUV flux of this magnitude is expected from an O or early B star within a distance of $\sim 1\text{ pc}$ of the protosun, and implies solar birth in a cluster of ~ 200 stars²², a very plausible birth scenario for our Solar System. The requirement of vigorous vertical mixing is consistent with theoretical predictions of the dynamics of disk instabilities^{20,25}. Our model makes two testable predictions. First, as pointed out by Clayton⁶, solar oxygen isotopes will be similar to the isotopically lightest CAIs ($\delta^{17}\text{O}_{\text{SMOW}} \approx \delta^{18}\text{O}_{\text{SMOW}} \approx -50\text{‰}$), a prediction that will be tested

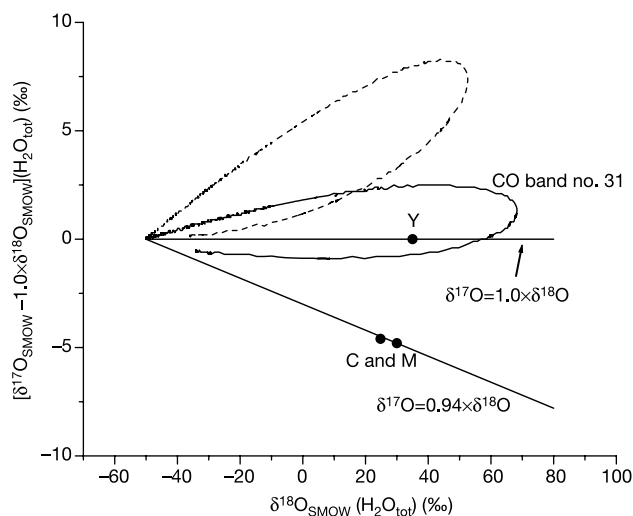


Figure 4 | Three-isotope plot of total nebular H_2O in the model, including an estimate of wavelength-dependent absorption by H_2 . The ordinate is $\delta^{17}\text{O} - 1.0 \times \delta^{18}\text{O}$, rather than $\delta^{18}\text{O}$, to emphasize differences in slope. The unlabelled curve (dashed line) is the same as the trajectory shown in Fig. 3. The solid curve includes differential shielding (that is, wavelength-dependent shielding) by H_2 on CO band number 31. CO band 31 accounts for $\sim 60\%$ of C^{18}O photodissociation in translucent molecular clouds¹⁰. Shielding functions that account for the differential shielding by H_2 on the isotopologues of CO band 31 were computed from H_2 synthetic spectra (see Supplementary Information). Differential shielding by H_2 brings the model δ -values for total nebular water within the range inferred from meteorites^{27,29}. The differential shielding analysis shown here applies to CO self-shielding in both the surface region of the disk and in the parent molecular cloud.

by analysis of solar wind samples returned by the GENESIS spacecraft. Second, H_2O in similarly irradiated protoplanetary disks will be enriched in ^{17}O and ^{18}O by $\sim 30\text{--}100\%$ relative to disk CO, a difference that will be measurable by the next generation of infrared and submillimetre telescopes (for example, SOFIA, Herschel and ALMA).

Received 27 December 2004; accepted 10 March 2005.

1. Clayton, R. N., Grossman, L. & Mayeda, T. K. Component of primitive nuclear composition in carbonaceous meteorites. *Science* **182**, 485–488 (1973).
2. Clayton, R. N. Oxygen isotopes in meteorites. *Annu. Rev. Earth Planet. Sci.* **21**, 115–149 (1993).
3. Thieme, M. H. & Heidenreich, H. E. Mass independent fractionation of oxygen: a novel isotope effect and its possible cosmochemical implications. *Science* **219**, 1073–1075 (1983).
4. Gao, Y. Q. & Marcus, R. A. Strange and unconventional isotope effects in ozone formation. *Science* **293**, 259–263 (2001).
5. Marcus, R. A. Mass-independent isotope effect in the earliest processed solids in the solar system: A possible chemical mechanism. *J. Chem. Phys.* **121**, 8201–8211 (2004).
6. Clayton, R. N. Self-shielding in the solar nebula. *Nature* **415**, 860–861 (2002).
7. Lyons, J. R. & Young, E. D. Towards an evaluation of self-shielding at the X-point as the origin of the oxygen isotope anomaly in CAIs. *Lunar Planet. Sci. Conf. XXXIV*, abstr. 1981 (2003).
8. Bally, J. & Langer, W. D. Isotope-selective photodissociation of carbon monoxide. *Astrophys. J.* **255**, 143–148 (1982).
9. Federman, S. R. *et al.* Further evidence for chemical fractionation from ultraviolet observations of carbon monoxide. *Astrophys. J.* **591**, 986–999 (2003).
10. van Dishoeck, E. F. & Black, J. H. The photodissociation and chemistry of interstellar CO. *Astrophys. J.* **334**, 771–802 (1988).
11. Yurimoto, H. & Kuramoto, K. Molecular cloud origin for the oxygen isotope heterogeneity in the solar system. *Science* **305**, 1763–1766 (2004).
12. Lyons, J. R. & Young, E. D. Evolution of oxygen isotopes in the solar nebula. *Lunar Planet. Sci. Conf. XXXV*, abstr. 1970 (2004).
13. Aikawa, Y. & Herbst, E. Two-dimensional distributions and column densities of gaseous molecules in protoplanetary disks. *Astron. Astrophys.* **371**, 1107–1117 (2001).

14. Allende Prieto, C., Lambert, D. L. & Asplund, M. A reappraisal of the solar photospheric C/O ratio. *Astrophys. J.* **573**, L137–L140 (2002).
15. Le Teuff, Y. H., Millar, T. J. & Markwick, A. J. The UMIST database for astrochemistry 1999. *Astron. Astrophys. Suppl. Ser.* **146**, 157–168 (2000).
16. Hasegawa, T. I., Herbst, E. & Leung, C. M. Models of gas-grain chemistry in dense interstellar clouds with complex organic molecules. *Astrophys. J.* **82**, 167–195 (1992).
17. Willacy, K., Klahr, H. H., Millar, T. J. & Henning, Th. Gas and grain chemistry in a protoplanetary disk. *Astron. Astrophys.* **338**, 995–1005 (1998).
18. van Zadelhoff, G. J., Aikawa, Y., Hogerheijde, M. R. & van Dishoeck, E. F. Axi-symmetric models of ultraviolet radiative transfer with applications to circumstellar disk chemistry. *Astron. Astrophys.* **397**, 789–802 (2003).
19. Markwick, A. J., Ilgner, M., Millar, T. J. & Henning, Th. Molecular distributions in the inner regions of protostellar disks. *Astron. Astrophys.* **385**, 632–646 (2002).
20. Stone, J. M., Gammie, C. F., Balbus, S. A. & Hawley, J. F. in *Protostars and Planets IV* (eds Manning, V., Boss, A. P. & Russell, S. S.) 589–611 (Univ. Arizona Press, Tucson, 2000).
21. Lee, H. H., Herbst, E., Pineau des Forêts, G., Roueff, E. & Le Bourlot, J. Photodissociation of H₂ and CO and time dependent chemistry in inhomogeneous interstellar clouds. *Astron. Astrophys.* **311**, 690–707 (1996).
22. Adams, F. C., Hollenbach, D., Laughlin, G. & Gorti, U. Photoevaporation of circumstellar disks due to external far-ultraviolet radiation in stellar aggregates. *Astrophys. J.* **611**, 360–379 (2004).
23. Young, E. D. & Russell, S. S. Oxygen reservoirs in the early solar nebula inferred from an Allende CAI. *Science* **282**, 452–455 (1998).
24. Cuzzi, J. N. & Zahnle, K. J. Material enhancement in protoplanetary nebulae by particle drift through evaporation fronts. *Astrophys. J.* **614**, 490–496 (2004).
25. Gammie, C. F. Layered accretion in T Tauri disks. *Astrophys. J.* **457**, 355–362 (1996).
26. Cuzzi, J. N., Dobrovolskis, A. R. & Hogan, R. C. in *Chondrules and the Protoplanetary Disk* (eds Hewins, R. H., Jones, R. H. & Scott, E. R. D.) 35–43 (Cambridge Univ. Press, Cambridge, 1996).
27. Clayton, R. N. & Mayeda, T. K. The oxygen isotope record in Murchison and other carbonaceous chondrites. *Earth Planet. Sci. Lett.* **67**, 151–161 (1984).
28. Choi, B. G., Krot, A. N., McKeegan, K. D. & Wasson, J. T. Extreme oxygen-isotope compositions in magnetite from unequilibrated ordinary chondrites. *Nature* **392**, 577–579 (1998).
29. Young, E. D. The hydrology of carbonaceous chondrite parent bodies and the evolution of planet progenitors. *Phil. Trans. R. Soc. Lond. A* **359**, 2095–2110 (2001).
30. Navon, O. & Wasserburg, G. J. Self-shielding in O₂: a possible explanation for oxygen isotope anomalies in meteorites? *Earth Planet. Sci. Lett.* **73**, 1–16 (1985).

Supplementary Information is linked to the online version of the paper at www.nature.com/nature.

Acknowledgements J.R.L. thanks K. McKeegan, J. Cuzzi and A. Boss for discussions, and P. Plavchan for assistance with IDL. J.R.L. acknowledges funding from the NASA Origins Program and from the UCLA Center for Astrobiology. E.D.Y. acknowledges support from the UCLA Center for Astrobiology.

Author Contributions J.R.L. conceived and carried out the calculations presented here, using a modified version of a photochemical code provided by J. Kasting. The paper was written by J.R.L. and E.D.Y.

Author Information Reprints and permissions information is available at npg.nature.com/reprintsandpermissions. The authors declare no competing financial interests. Correspondence and requests for materials should be addressed to J.R.L. (jrl@ess.ucla.edu).